NASA Contractor Report 181717

ICASE REPORT NO. 88-54

ICASE

AN ADAPTIVE PSEUDOSPECTRAL METHOD FOR DISCONTINUOUS PROBLEMS

Jeffrey M. Augenbaum

Contract No. NAS1-18107
September 1988

(NASA-CR-181717) AN ADAPTIVE PSEUDOSPECTRAL METHOD FOR DISCONTINUOUS PROBLEMS Final Report (NASA) 34 p CSCL 12A

N89-10583

Unclas
G3/64 0168486

INSTITUTE FOR COMPUTER APPLICATIONS IN SCIENCE AND ENGINEERING
NASA Langley Research Center, Hampton, Virginia 23665

Operated by the Universities Space Research Association

National Aeronautics and
Space Administration

Langley Research Center
Hampton, Virginia 23665

An Adaptive Pseudospectral Method for Discontinuous Problems

Jeffrey M. Augenbaum *
Department of Mathematics, U-9
University of Connecticut
Storrs, CT 06268

Abstract

In this paper, we study the accuracy of adaptively chosen, mapped polynomial approximations for functions with steep gradients or discontinuities. We show that, for steep gradient functions, one can obtain spectral accuracy in the original coordinate system by using polynomial approximations in a transformed coordinate system with substantially fewer collocation points than are necessary using polynomial expansion directly in the original, physical, coordinate system. We also show that one can avoid the usual Gibbs oscillation, associated with steep gradient solutions of hyperbolic pde's, by approximation in suitably chosen coordinate systems. Continuous, high gradient, solutions are computed with spectral accuracy (as measured in the physical coordinate system). Discontinuous solutions associated with nonlinear hyperbolic equations can be accurately computed by using an artificial viscosity chosen to smooth out the solution in the mapped, computational, domain. Thus, we can effectively resolve shocks on a scale that is subgrid to the resolution available with collocation only in the physical domain. Examples with Fourier and Chebyshev collocation are given.

*Research was supported by a University of Connecticut Research Foundation Faculty Research award and by the National Aeronautics and Space Administration under Contract No. NAS1-18107 while in residence at the Institute for Computer Applications in Science and Engineering (ICASE), NASA Langely Research Center, Hampton, VA 23665.

1 Introduction

During the past decade, spectral methods have become the numerical method of choice for the approximate solution of time dependent partial differential equations in many branches of computational science. This is due to their ability to yield highly accurate approximations of smooth solutions with substantially fewer grid points than would be required by comparative finite difference methods. Thus, for complex flows requiring detailed simulation, the success of spectral methods has been striking. This is particularly true for simulation of turbulent flows and the transition to turbulence (see references in [8]). Spectral methods have also become the primary numerical method in global weather modeling [14,18].

Straight forward application of the spectral method to problems with highly localized phenomena that are not well resolved by the global discretization produce incorrect, globally oscillating, solutions due to the Gibbs phenomenon [8,11,27]. This phenomenon shows up in linear and nonlinear equations and includes both computational discontinuities (continuous solutions with steep gradients that are not resolved by the finite discretization) and real discontinuities (such as shock waves). Various methods [1,8,9,10,12,16,17,20,23] have been proposed to extract the correct physical solution from the unwanted oscillatory one. Most of these add a finite order truncation error. A spectrally accurate physical space filter [1,9,12] and a spectrally accurate vanishing viscosity [22,26] have been demonstrated. Both of these approaches, however, perform poorly when used with a realistic number of collocation points. More sophisticated, nonoscillatory spectral methods are currently under investigation [7].

Adaptive grid methods have been used successfully with finite difference and finite element methods for many problems with highly localized phenomenon (see references in [2]). The dynamic placement of points to increase local resolution in adaptive finite difference and finite element methods is not applicable to spectral methods since the location of the collocation points for pseudospectral methods is intimately connected with the global convergence properties of the polynomial approximation. (The accuracy of polynomial expansions for various choices of collocation points is investigated in [25].)

An alternative approach to achieving high resolution locally is to use coordinate transformations which stretch out the region of high gradients so that, in the new coordinate system, the high gradient phenomena is well resolved. One can then use standard spectral methods to solve the mapped equation in the new coordinate system. Such a technique has been successfully applied to a system of reaction diffusion equations arising in combustion in [4,5] and independently in [13].

By using adaptively chosen coordinate transformations and computing in the computational domain, we are no longer using polynomial approximation for the solution in the physical coordinate system. In this paper, we examine the accuracy of mapped polynomial approximations. We shall see that, for steep gradient functions, one can obtain spectral accuracy in the physical space by using polynomial approximation in a transformed coordinate system with substantially fewer collocation points than would be necessary with polynomial approximation directly in the physical space. We also show that one can avoid the usual Gibbs oscillation associated with discontinuous solutions of hyperbolic pde's, by approximation in suitably chosen coordinate systems. Continuous, high gradient solutions are computed with spectral accuracy (as measured in the physical coordinate system). Discontinuous solutions associated with nonlinear hyperbolic equations can be accurately computed by using an artificial viscosity chosen to smooth out the solution in the computational domain where the solution is already more smoothly represented than in the physical domain. Thus, we effectively resolve the shock on a scale that is subgrid to the resolution available with collocation only in the physical domain.

In the next section, we describe the adaptive spectral method and present numerical experiments in section 3. Conclusions are presented in section 4.

2 Numerical Method

Review of Standard Pseudospectral Method

We illustrate the standard pseudospectral method [8,11,27] by considering the one dimensional equation

$$u_t = G(u) \tag{1}$$

where G is a differential operator on the interval $x \in [a,b]$. The function u(x,t) is approximated (suppressing the time dependence) by a polynomial

$$P_N u(x) = \sum_{j=0}^{N} a_j \psi_j(x) \tag{2}$$

that interpolates u(x) at N+1 distinct points $x_0, \ldots x_N$ at time t. At the collocation points x_k, if $\psi_j(x_k) = \delta_{jk}$, then $a_j = u(x_j)$. The expansion polynomial then has the form

$$u_N(x) = P_N u(x) = \sum_{j=0}^{N} u(x_j) \psi_j(x) \tag{3}$$

where $\psi_j(x_k) = \delta_{jk}$. Differentiation of u is accomplished by analytically differentiating the interpolating polynomial

$$\partial u_N/\partial x = \sum_{j=0}^{N} u(x_j)\psi_j'(x) \tag{4}$$

Hence, given the values of u(x) at the collocation points x_k, we can find the approximate derivative (at the collocation points) by a matrix D multiplying the grid function $u(x_k)$. D can be computed explicitly from $D = \{d_{jk}\} = \psi_j'(x_k)$. The cost of computing the derivative is $O(N^2)$ operations from the matrix multiplication. This can be very efficient on a vector or parallel computer. Higher derivative matrices can easily be constructed from the relation $D_k = (D)^k$. Boundary conditions can also be directly incorporated into the differentiation matrices.

Common choices for collocation points and interpolating polynomials [8,27] are the fourier collocation points

$$x_j = \frac{2\pi j}{N+1} \qquad j = 0, \ldots, N\ (N odd)$$

with

$$\psi_j(x) = \frac{1}{N+1}\sin[\frac{(N+1)(x-x_j)}{2}]\cot[\frac{x-x_j}{2}] \tag{5}$$

for periodic problems in $x \in [0, 2\pi]$, and the Chebyshev collocation points

$$x_j = \cos \pi j/N \qquad j = 0, \ldots, N$$

with

$$T_n(x) = \cos(n \cos^{-1}(x))$$

and

$$\psi_j(x) = \frac{(-1)^{j+1}(1-x^2)T_N'(x)}{c_j N^2 (x - x_j)} \tag{6}$$

where $c_0 = c_N = 2$, and $c_j = 1$,for $1 \leq j \leq N-1$ for nonperiodic problems in $x \in [-1, 1]$.

These particular choices enable the interpolating polynomials to also be written as an expansion in orthogonal basis functions $\{\phi_j(x)\}$ such that the sums (3) and (4) can be computed by an FFT. This reduces the cost of computing the spectral derivative from $O(N^2)$ to $O(N \log N)$ operations. The matrix multiplication, however, has the advantage that it is more flexible and easier to vectorize.

Thus, the pseudospectral approximate solution $u_j = u(x_j, t)$ at time t=t^{n+1} is obtained by first evaluating the differential operator G at the collocation points at time t=t^n by either an FFT or a matrix multiplication, and then updating (in time) the resulting system of ordinary differential equations.

Description of Adaptive Procedure

We now describe the adaptive procedure (first introduced in [5] for a system of reaction diffusion equations modeling solid fuel combustion).

A family of transformations

$$s = q(x, \overline{\alpha}) \tag{7}$$

mapping the interval [a,b] onto itself, and parameterized by the vector $\overline{\alpha}$, is introduced. Each value of $\overline{\alpha}$, defines a new coordinate system to which equation (1) can be transformed and then solved by the standard pseudospectral method (in the new coordinate system). In the experiments described below we use coordinate transformations with two degrees of freedom. One parameter β controls the magnitude of the coordinate stretching (or compression) about a point determined by the second parameter γ . For periodic problems we map the physical x coordinate system ($x \in [0, 2\pi]$) to the computational s coordinate system ($s \in [0, 2\pi]$) with the fractional linear transformation

$$e^{is} = \frac{e^{i(x-\gamma)} - \beta}{1 - \beta e^{i(x-\gamma)}} \tag{8}$$

where $|\beta| < 1$ and $0 \leq \gamma \leq 2\pi$. For nonperiodic problems, we map the physical coordinates, $x \in [-1, 1]$, to the computational coordinates, $s \in [-1, 1]$, with the composite transformation

$$s = \frac{2}{\pi} tan^{-1}[\frac{1}{\beta} tan[\frac{\pi}{2}(\frac{\gamma + x}{\gamma x + 1})]]. \tag{9}$$

where $\beta > 0$, and $|\gamma| < 1$. In both cases, the mappings are analytic and easily inverted and differentiated.

Differentiation matrices are easily constructed for the collocation points in the computational domain since $\partial u/\partial x = \partial/\partial s \frac{ds}{dx} = q' \partial/\partial s \approx QD = \tilde{D}$, where Q is a diagonal matrix whose elements contain the derivative of the map, and D is the differentiation matrix for the collocation points in the physical domain. Higher derivatives are obtained by taking powers of $\tilde{D}$. The transformed equations can be easily generated with the matrix formulation, making the exact representation in a particular coordinate system transparent. We simply interpolate u(x,t) to u(s,t) and use $\tilde{D}$ instead of D in (1).

A particular coordinate system for a function u(x) can be found by minimizing a two parameter functional bounding the interpolation error in the maximum norm. The pointwise interpolation error

$$|u(x) - u_{N-1}(x)| = |\sum_{j=N}^{\infty} \hat{u}_j \phi_j(x)| \tag{10}$$

can be reduced by finding a coordinate system in which the leading term in the interpolation error is minimized. In the nonperiodic case, this leads to the functional derived in [4]

$$I(\overline{\alpha}) = \int_{-1}^{1} [(\sqrt{1-s^2}\frac{d}{ds})^2 u]^2 \frac{ds}{\sqrt{1-s^2}}. \tag{11}$$

In the periodic case, a similar derivation (see Appendix), leads to the H^1 norm

$$I(\overline{\alpha}) = \int_0^{2\pi} [|u_s|^2 + |u|^2] ds. \tag{12}$$

We will also consider the effects of using the H_2 norm,

$$I(\overline{\alpha}) = \int_0^{2\pi} [A|u_{ss}|^2 + B|u_s|^2 + C|u|^2] ds. \tag{13}$$

The algorithm is therefore:
i) discretize the right hand side of (1) and integrate the resulting ODE's to $t = t_1$ in an initial coordinate system.
ii) find $\overline{\alpha}_{min}$ which minimizes the monitor function $I(\overline{\alpha})$.
iii) Interpolate the solution to the collocation points in the new coordinate system using the interpolation formula (3).
iv) Integrate to $t = t_2$.
v) go to (ii).

3 Numerical Experiments

In this section we consider the efficiency and accuracy of mapped polynomial expansions. We study applications to approximation theory and hyperbolic partial differential equations. Using the previously described adaptive procedure, a function is approximated by orthogonal polynomials in some transformed coordinate system 's'. However, we measure the accuracy by computing the error in the original 'physical' coordinate system.

Approximation Theory

We measure the approximation error by considering the pointwise error at a sequence of points. Since the error at the collocation points is zero by construction, we interpolate to a sequence of N' uniformly spaced points, y_j. The pointwise error is given by

$$e(y_j) = |f(y_j) - f_N(y_j)| \qquad j = 0, \ldots, N' \tag{14}$$

where $f_N(x)$ is a polynomial of degree N. Next we minimize the monitor function and determine a coordinate system, s. We then represent $f(s)$ *at the collocation points in the*

new coordinate system and interpolate to the points $s_j = s(y_j)$, the image of the points y_j. The pointwise error is again measured in the original 'x' coordinate system.

In figure 1a, we display the log of the maximum pointwise error for $f(x) = tanh(Mx)$ with M = 8, 16, 32 in the interval $x \in [-1,1]$. We approximate $f(x)$ by Chebyshev polynomials of degree N, where N/M = 1,..,4. The top three graphs are the result of standard Chebyshev polynomial approximation, while the bottom three are the result of Chebyshev polynomial approximation in a coordinate system selected by the minimization of the monitor function (11). Although both cases converge exponentially, we see the mapped polynomials require considerably fewer points to achieve very high accuracy. Since the high gradient region occurs in the center of the domain, simply adding Chebyshev collocation points provides increasing resolution faster at the boundaries than at the center. Therefore it is more effective to use the coordinate stretching to increase local resolution than to simply add more collocation points in the original coordinate system. The adaptive procedure provides a coordinate stretching where the gradient is largest and maps it to a coordinate system where a significant proportion of the collocation points contribute to its resolution.

Next, we examine the convergence properties of the adaptive method when the steep gradient region varies away from the center of the domain, where the resolution is coarsest, to the boundary, where the resolution is finest. In figure 1b. we show the log of the maximum pointwise error for $f(x) = tanh[M(x - x_0)]$ with M = 8,32,128 and x_0 varying between the center ($x_0 = 0$) and the boundary ($x_0 = 1$). In this case we use Chebyshev expansion with 32 modes. For a given value of M, the top plot is the standard Chebyshev polynomial and the bottom plot is the mapped polynomial interpolation. We see that for M = 8 and 32 the error is several orders of magnitude smaller with the mapped polynomial expansions than with the standard Chebyshev polynomial interpolation. However for M=128, there is insufficient resolution to resolve the gradient even with the mapping; and hence the errors are only slightly better with the mapping. The oscillation in the adaptive cases is due to the fact that in the discrete search of parameter space (β, γ) to find a minimum for (11) we only looked at values of γ that were multiples of .1, whereas the point of maximum gradient (x_0) was allowed to vary in multiples of .05. Thus, when x_0 occurs between multiples of .1, the optimal parameters were not found. Still the results are much better than if no mapping had taken place.

Partial Differential Equations

In the previous section, we have shown that for functions with large gradients, mapped polynomials can yield several orders of magnitude more accuracy than the standard spec-

tral expansions. We now consider the accuracy of mapped polynomial expansions in the context of hyperbolic partial differential equations where the coordinate transformations can vary dynamically in time. We consider several prototype examples of wave propagation including a linear wave equation for advection of a sharp spike and the nonlinear Burgers equation for shock formation and propagation. In both cases we will consider periodic boundary conditions and hence we use triginometric polynomials for the spatial discretization. In order to control the temporal errors in all of our examples we use the LSODE solver from the ODEPACK package [6,15] to integrate the resulting system of (spatially discretized) ordinary differential equations. This solver uses dynamically chosen time stepping in order to guarantee a prescribed error tolerance at each output time. The error tolerance was set to 10^{-7}.

In practice we do not change coordinate systems every time step. Instead, we evaluate the monitor function $I(\overline{\alpha})$ at each time step and compare it with its previous value when we last changed coordinate systems. We adapt to a new coordinate system when the ratio falls below .7 or above 1.3 .

Linear Hyperbolic Equations

Consider the one dimensional linear advection equation

$$u_t + u_x = 0 \tag{15}$$

with periodic boundary conditions on the interval $0 \leq x \leq 2\pi$. Nonsmooth initial data u(x,0)=f(x) yields the nonsmooth solution u(x,t)=f(x-t) (extended periodically) for all $t > 0$. We choose a sharply peaked Gaussian initial function

$$f(x) = e^{-(x-\pi)^2/4\Delta x^2} \tag{16}$$

This yields a Gaussian with width $2\Delta x$, where $\Delta x = 2\pi/N$. If we choose $4\Delta x^2 = .025$ then $\Delta x = .078$, corresponding to $N = 2\pi/\Delta x \approx 80$ points. Thus we need a local resolution corresponding to N=80 points near the peak. In our example we will use 32 points, therefore the function is not adequately resolved near the peak and behaves as if there is a discontinuity. We expect to see global oscillations. In figure 2a, we display the computed solution at time t= 0, 15, 30, 45, 60, 64 Δt. In these examples we use a time step of $\Delta t = .5\Delta x$, and integrate in time with an explicit Adams scheme from the LSODE package (MF=10). Note that the LSODE package uses an internally chosen Δt to guarantee the prescribed accuracy. Thus Δt is only used for output purposes. We see that when the solution is not centered at a grid point, the spectral approximation displays high frequency oscillations. This could have a serious effect in more complicated

systems where the advected quantity is then fed into other components of the system. We also point out the observation that the information about the correct physical solution is still contained in the oscillatory solution; and the spectral method is able to accurately reproduce the solution in future time, when the spike is centered at a grid point. The explanation for this is due to the fact that since the interpolation error of the initial function is constructed to vanish at the collocation points, and since the spectral method introduces almost no dissipation, whenever the solution is merely a translate of the initial function to a center about another collocation point it displays no interpolation error. Hence we can reproduce, without oscillation, the exact solution at the collocation points at times when Δt is a integer multiple of Δx. At other times when the solution is a translate of the initial function between collocation points, we observe the expected global oscillation.

In the adaptive case, we begin by chosing an appropriate coordinate system to adequately represent the initial function. We therefore minimize the H^1 norm of the initial function (16), which we assume to have with as much resolution as needed. The initial function is then prescribed at the N fourier collocation points in the new coordinate system. The transformed equation

$$u_t + (x_s)u_s = 0 \tag{17}$$

is then updated by the standard fourier collocation method. This procedure is then repeated every time step, with the adaption occurring as described previously. In figure 2b, we display the results of the computation, based on adaption with the H^1 norm, at the same output times as in the non-adaptive case (figure 2a.). For output purposes, we have interpolated the solution back to the physical x coordinate system. In figure 2c, the same computation was done using the H^2 norm of u as the minimizing functional. We also present, in figure 2d, for comparison, results of the adaptive procedure with the spatial differentiation matrix replaced with the fourth order finite difference matrix.

We compare these cases by computing the l_2 errors of the grid functions ie

$$\|e(t)\|_2 = \{\frac{1}{N}\sum_{j=0}^{N} |u_{exact}(x_j,t) - u_{computed}(x_j,t)|^2\}^{1/2} \tag{18}$$

and the l_∞ error

$$\|e(t)\|_\infty = max_j|u_{exact}(x_j,t) - u_{computed}(x_j,t)|. \tag{19}$$

The maximum time errors

$$\max_{t\in[0,2\pi]} \|e(t)\|_{2,\infty}$$

for the four schemes is presented in table 1.

Method	*max l_2 error*	*max l_∞ error*
Standard fourier collocation	.038	.096
Adaptive fourier collocation using H^2 norm	.003	.009
Adaptive fourier collocation using H^1 norm	.006	.012
Adaptive 4-th order finite diff. using H^2 norm	.143	.446

These results suggests that adaption based on minimizing the H^2 norm is preferred over adaption based on the H^1 norm. When the sole criteria for choosing the coordinate system is the H^1 norm too much weight is placed on the steep gradient (high frequency) region of the solution at the expense of the smooth (low frequency) region. We can see in figure 2b, the presence of a low frequency error component in the smooth, constant, portion of the solution. The use of the H^2 norm provides a smoother coordinate mapping with more emphasis on the smooth region of the solution. Thus, the low frequency components of the solution is more accurate. Both adapted solutions, however, provide significant improvement over the nonadapted solution and the adapted fourth order finite difference solution.

Nonlinear Hyperbolic Equations

As a model for the formation of discontinuous solutions, we consider Burgers equation

$$u_t + \frac{1}{2}(u^2)_x = 0 \tag{20}$$

with periodic boundary conditions on the interval $0 \leq x \leq 2\pi$. Smooth initial data u(x,0)=f(x) will develop discontinuous (weak) solutions in finite time. An entropy condition is required to pick out the correct *physical* solution [21].

The fourier collocation method will break down and yield global oscillations as soon as the solution steepens up too much to be resolved on the finite grid. The adaptive procedure will delay this breakdown, but its occurrence is inevitable. Artificial viscosity can smooth out the solution so that it becomes resolvable on the finite grid. This introduces a finite order truncation error and therefore we loose the spectral accuracy. Recently [22,26], a spectrally accurate vanishing viscosity solution has been shown to converge to the entropy solution of (20). However, computations with realistic number of collocation points still shows global oscillations [26].

We propose here to couple the adaptive pseudospectral method with the artificial viscosity method to produce oscillation free solutions using significantly less artificial viscosity than would be necessary with standard fourier collocation. This will reduce the truncation error introduced by the artificial viscosity. Gottlieb et al. [10] have shown that spectral collocation methods are capable of resolving a shock over one effective grid interval. We

therefore expect, that by appropriate coordinate stretching, the adaptive pseudospectral method can resolve shocks over a significantly smaller effective grid interval; the equivalent of using several times more collocation points.

We approximate the solution of the inviscid Burgers equation (20) by the viscous version

$$u_t + \frac{1}{2}(u^2)_x = \nu u_{xx} \tag{21}$$

where νu_{xx} is the artificial viscosity term, and ν is a grid dependent viscosity coefficient. It is well known [21], that in the limit $\nu \downarrow 0$ solutions of (21) converge to the entropy solution of (20). In our numerical experiments we use initial data f(x) = sin(x). The inviscid Burgers equation develops a shock discontinuity at $x = \pi$. Again, the fourier collocation differentiation matrix is used for the spatial differentiation. The resulting system of ODE's was integrated using an explicit Adams method (MF=10) from the LSODE package. The solution was integrated up to time $t = 1.47$, after the shock has formed. We determined experimentally that for collocation with 32 points, a viscosity of $\nu = .08$ is needed to obtain an oscillation free solution. The adaptive solution based on the H^1 norm only needs a viscosity coefficient of $\nu = .02$ to yield an oscillation free solution. In figures 3a,b,c we show a) a time history of the solution up to t=1.47, b) the exact and computed solutions at t=1.47 and c) a time history of the errors for the non adaptive fourier collocation solution of (21) with artificial viscosity coefficients of $\nu = .08$. In figure 4a,b,c we show the same plots for the adapted solution with an artificial viscosity coefficient $\nu = .02$.

Comparing the two cases we see the non adapted solution requires four times as much viscosity to reduce the global oscillations. The effect of this larger viscosity can be seen in a much larger region about the shock and, in fact, prevents the computed solution from shocking up. The maximum error occurs just before the solution shocks up, when the second derivative is greatest. The smaller viscosity used in the adaptive solution accounts for a reduction in the maximum pointwise error by a factor of four. The larger viscosity needed for the nonadaptive solution prevents the solution from steepening any further, and the maximum pointwise error persists after the shock forms. However the adapted solution, with the smaller viscosity, is able to steepen further and approach the true shock solution. After the shock forms, the solution is essentially piecewise linear and the effect of the second derivative truncation error is reduced. The error is then reduced another factor of four.

Finally, we consider the case of a moving shock. If we use the initial condition $f(x) = .3 + .7sin(x)$, the solution shocks up and starts starts to propagate. In figure 5a, we plot a sampling of the time history of the solution up to t=4.1. The pointwise error at these sampled times are plotted in figure 5b. As in the previous case, we use adaption

based on the H^1 norm and a viscosity coefficient of $\nu = .02$. We see that, as before, the maximum pointwise errors occurrs just before the solution shocks up, when its curvature is maximum. After the solution shocks up it almost piecewise linear and the truncation error due to viscosity is reduced. The solution then propagates without exhibiting global oscillations. Subsequent peaks in the errors (displayed in 5b) is due to the discrete search of parameter space in the minimization of the monitor function (12). More sophisticated minimization routines will be used in the future.

4 Conclusions

We have demonstrated that mapped polynomial approximation can provide significant improvements in accuracy and efficiency for approximating functions with steep gradients.

Using analytic, dynamically varying, simple coordinate transformations we achieve improvements in convergence of several orders of magnitude for continuous functions with steep gradients. These results are robust in the sense that even with crude minimization procedures, that don't find the optimal coordinate transformation, we achieve significant improvements over the nonadapted case.

Discontinuous functions require smoothing in addition to coordinate transformations. In this work we have used artificial viscosity to provide the smoothing. Although this adds a finite order truncation error, the effects are greatly reduced by computing in the transformed coordinate system where less artificial viscosity is needed. Artificial viscosity does have the drawback that it reduces the allowable time step for explicit methods from $O(N^2)$ to $O(N^4)$ for Chebyshev based collocation. We are currently working with alternate smoothers based on filtering the expansion coefficients in spectral space [10,23]. These results will be reported elsewhere.

In this paper, we have restricted our attention to problems with only one high gradient region. Problems with multiple steep gradient regions can be treated using more complicated mapping functions. This will increase the dimensionality of parameter space searched in the minimization of the monitor function. A better approach is to couple the adaptive spectral method with a multidomain approach [19,24] so that the simple mappings described above can be used in each domain. We are currently investigating this approach.

Acknowledgements

The author would like to thank Alvin Bayliss, David Gottlieb and Yvonne Maday for several stimulating discussions. Computing resources were provided by a supercomputer time allocation grant at the National Center for Supercomputer Applications, University of Illinois at Urbana-Champaign and by the Mathematics Computing Lab, University of Connecticut.

Appendix A

We now derive a bound for the maximum norm of the interpolation error of a periodic function. Using the standard notation, we represent a periodic function u(x) as an expansion of triginometric basis functions

$$u(x) = \sum_{k=-\infty}^{\infty} a_k e^{ikx} \tag{22}$$

where

$$a_k = \frac{1}{2\pi}\int_0^{2\pi} u(x)e^{-ikx}dx, \quad |k| = 0,1,2,.. \tag{23}$$

If we use the the galerkin approximation of u(x),

$$u_N(x) = P_N u(x) = \sum_{k=-N}^{N} a_k e^{ikx} \tag{24}$$

then the pointwise error is

$$|u(x) - u_{N-1}(x)| = |\sum_{|k|\geq N} a_k e^{ikx}|. \tag{25}$$

We can now bound the spectral interpolation error in the maximum norm by

$$max_{0\leq x<2\pi}|u(x) - u_{N-1}(x)| \leq \sum_{|k|\geq N} |a_k|. \tag{26}$$

Applying integration by parts to (23) p times and noting the periodicity of the boundary conditions, we have

$$a_N = \frac{1}{2\pi}\frac{(-1)^{p+1}}{(iN)^p}\int_0^{2\pi} u^{(p)}e^{-iNx}dx, \quad p = 1,2,\ldots \tag{27}$$

We can bound a_N by applying the Cauchy-Schwartz inequality to (27)

$$|a_N| \leq \frac{1}{N^p}\{\int_0^{2\pi} |u^{(p)}|^2 dx\}^{\frac{1}{2}} \quad p = 1,2,\ldots \tag{28}$$

It is therefore reasonable to use the functional

$$I(\overline{\alpha}) = \int_0^{2\pi} A|u_{ss}|^2 + B|u_s|^2 + C|u|^2 ds \tag{29}$$

as the measure for the interpolation error in a coordinate system s.

Although this is the same functional used in [5,13] for Chebyshev polynomial approximation, the estimates leading to (29) in that case are not sharp. In fact, (29) was reported in [4] to not be sufficiently sensitive to variations in the behavior of the solution. When dealing with periodic functions, however, the same type of sharp estimates that lead to the alternate functional used in [4], here lead to the H^p norm functionals (eqs. (12) and (13)), as used originally in [5,13].

References

[1] Abarbanel, S., Gottlieb, D., and Tadmor, E.; *Spectral methods for discontinuous problems* in Numerical Methods for Fluid Dynamics, ed. by K. W. Morton and M. J. Baines, Oxford University Press (1986), pp. 129-153.

[2] Babuska, I., Chandra, J., and Flaherty, J.; *Adaptive Computational Methods for Partial Differential equation*, SIAM, (1984).

[3] Basdevant, C., Deville, M., Haldenwang, P., Lacroix, J., Orlandi, D., Quazzani, J., Patera, A., and Peyret, R.; *Spectral and finite difference solutions of the Burgers equation*, Computers and Fluids **14** (1986), pp. 23-41.

[4] Bayliss, A., Gottlieb, D., Matkowsky, B., and Minkoff, M.; *An adaptive pseudospectral method for reaction diffusion problems*, ICASE report No. 87-67 (1987), 40 pages.

[5] Bayliss, A. and Matkowsky, B.; *Fronts, relaxation oscillations and period doubling in solid fuel combustion*, J. Comp. Phys. **71** (1987), pp. 147-168.

[6] Byrne, G. D. and Hindmarsh, A. C.; *Stiff ODE solvers: A review of current and coming attraction*, J. Comp. Phys. **70** (1987), pp. 1-62.

[7] Cai, W., Gottlieb, D., and Shu, C. W.; *Non-oscillatory spectral fourier methods for shock wave calculations*, ICASE report No. 88-37 (1988), 31 pages.

[8] Canuto, C., Hussaini, M. Y., Quarteroni, A., and Zang, T. A.; *Spectral Methods in Fluid Dynamics*, Springer-Verlag (1988), 512 pages.

[9] Gottlieb, D.; *Spectral methods for compressible flow problems* in Proc. 9th Int. Conf. Numerical Methods in Fluid Dynamics, ed. by Soubbarameyer, J. P. Boujot, Springer-Verlag (1985), pp. 48-61.

[10] Gottlieb, D., Lustman, L., and Orszag, S.; *Spectral calculations of one-dimensional inviscid compressible flows*, SIAM J. Sci. Stat. Comput. **2** (1981), pp. 296-310.

[11] Gottlieb, D. and Orszag, S.; *Numerical Analysis of Spectral Methods: Theory and Applications*, SIAM (1977).

[12] Gottlieb, D. and Tadmor, E.; *Recovering pointwise values of discontinuous data within spectral accuracy*, in Progress and Supercomputing in Computational Fluid Dynamics, ed. by E. M. Murman and S. Abarbanel, Birkhauser (1985), pp. 357-375.

[13] Guillard, H. and Peyret, R.; *On the use of spectral methods for the numerical solution of stiff problems*, Comp. Meth. App. Mech. Eng. **66** (1988), pp. 17-43.

[14] Haltiner, G. J. and Williams, R. T.; *Numerical Prediction and Dynamic Meteorology*, John Wiley and Sons (1980).

[15] Hindmarsh, A. D.; *ODEPACK, a systematized collection of ODE solvers*, in Scientific Computing, ed. by R. S. Stepleman et al., North Holland (1983), pp. 55.

[16] Hussaini, M. Y., Kopriva, D., Salas, M. D., and Zang, T. A.; *Spectral methods for the Euler equations, part 1: Fourier methods and shock capturing*, AIAA J. **23** (1985), pp. 64-70.

[17] Hussaini, M. Y., Kopriva, D., Salas, M. D., and Zang, T. A.; *Spectral methods for the Euler equations, part 2: Chebyshev methods and shock fitting*, AIAA J. **23** (1985), pp. 234-240.

[18] Jarraud, M. and Baede, A. P. M.; *The use of spectral techniques in numerical weather prediction*, in Large Scale Computations in Fluid Mechanics, Lectures in Applied Mathematics **22** (1985), pp. 1-41.

[19] Kopriva, D.; *A spectral multidomain method for the solution of hyperbolic systems*, Appl. Numer. Math. **2** (1986), pp. 221-241.

[20] Kopriva, D.; *A practical assessment of spectral accuracy for hyperbolic problems with discontinuity*, J. Sci. Computing **2** (1987), pp. 249-262.

[21] Lax, P. D.; *Hyperbolic Systems of Conservation Laws and the Mathematical Theory of Shock Waves*, SIAM Regional Conference Lectures in Applied Mathematics, No. 11 (1972).

[22] Maday, Y. and Tadmor, E.; *Analysis of the spectral vanishing viscosity method for periodic conservation laws*, ICASE Report No. 88-4 (1988), 34 pages.

[23] Majda, A., McDonough, J., and Osher, S.; *The fourier method for nonsmooth initial data* , Math. Comp. **32** (1978), pp. 1041-1081.

[24] Macaraeg, M., and Street, C. L.; *Improvements in spectral collocation through a multiple domain technique*, Appl. Numer. Math. **2** (1986), pp. 95-108.

[25] Solomonoff, A. and Turkel, E.; *Global collocation methods for approximation and the solution of partial differential equations*, ICASE Report No. 86-60 (1986), 65 pages.

[26] Tadmor, E.; *The convergence of spectral methods for nonlinear conservation laws*, ICASE Report No. 87-54 (1987), 21 pages.

[27] Voigt, R., Gottlieb, D., and Hussaini, M. Y., ed. *Spectral Methods for Partial Differential Equations*, SIAM (1984), 267 pages.

Figure Captions

Figure 1a. Log of pointwise error for $f_N(x) \approx tanh(Mx)$ where $\frac{N}{M} = 1, 2, 3, 4$.

Figure 1b. Log of maximum pointwise error for $f_{32}(x) \approx tanh[M(x - x_0)]$. M = 8,32,128 and $0. \leq x_0 \leq 1$.

Figure 2a. Computed solution for the linear advection equation (15) with 32 collocation points at time t = 0,15,30,45,60 and 64 Δt, with $\Delta t = .5(\frac{2\pi}{32})$.

Figure 2b. Same as (2a) except solution adaptively computed based on H^1 norm.

Figure 2c. Same as (2a) except solution adaptively computed based on H^2 norm.

Figure 2d. Same as (2a) except solution adaptively computed based on H^2 norm and fourth order spatial differentiation is used.

Figure 3a. Time history for viscous nonadapted Burger equation up to t=1.47. Viscosity coefficient is $\nu = .08$.

Figure 3b. Computed and exact solution at time t = 1.47.

Figure 3c. Pointwise error history for solution displayed in 3a.

Figure 4a. Time history for adaptively computed viscous Burger equation up to t = 1.47. Viscosity coefficient is $\nu = .02$.

Figure 4b. Computed and exact solution at time t = 1.47.

Figure 4c. Pointwise error history for solution displayed in 4a.

Figure 5a. Sampling of time history for adaptively computed viscous Burger equation up to t = 4.1. Viscosity coefficient is $\nu = .02$. Initial function $u(x) = .3 + .7sin(x)$

Figure 5b. Pointwise error history for solution displayed in 5a.

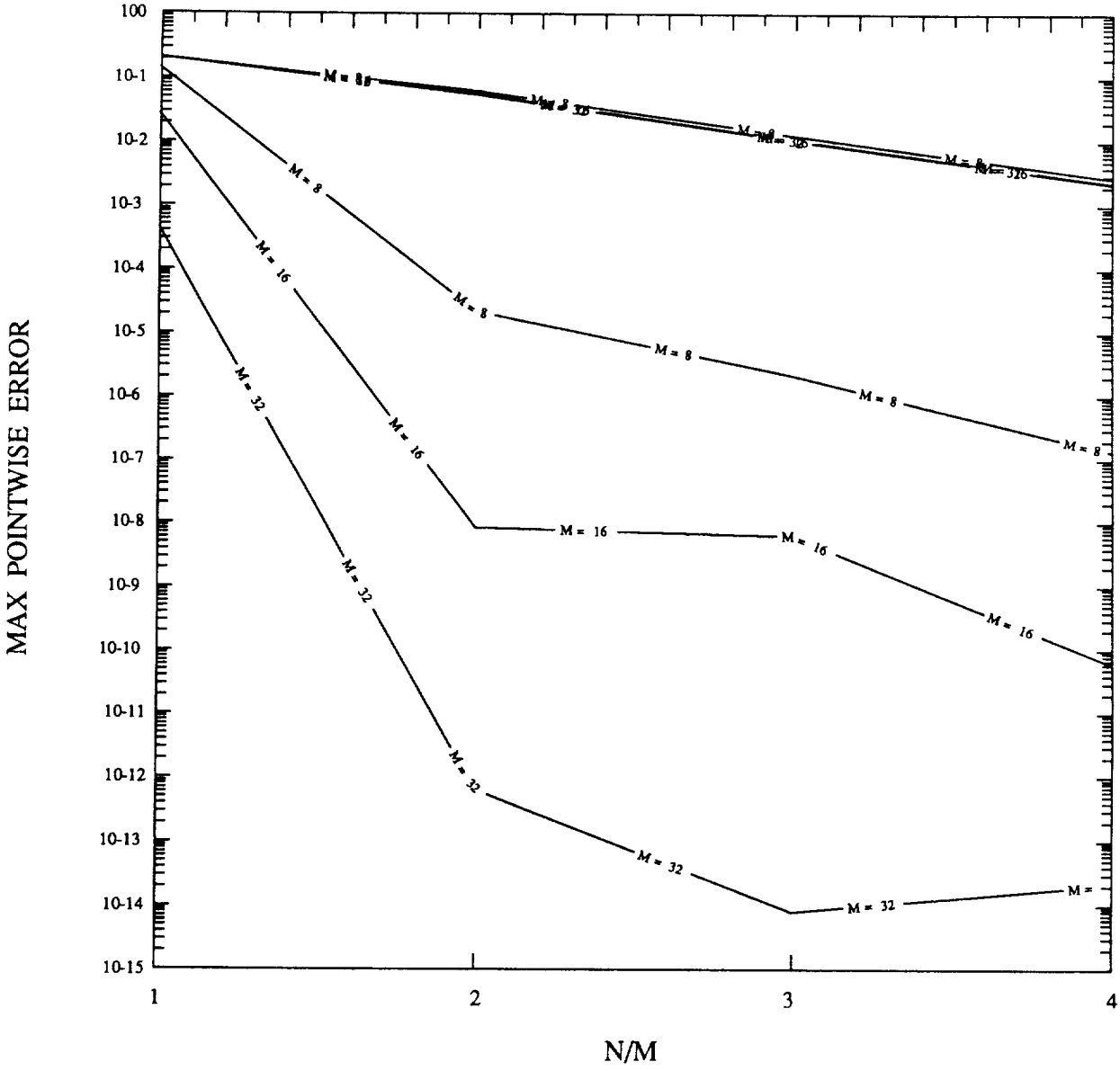
MAX POINTWISE ERROR
100
10-1
10-2
10-3
10-4
10-5
10-6
10-7
10-8
10-9
10-10
10-11
10-12
10-13
10-14
10-15
1
2
3
4
N/M
M = 8
M = 16
M = 32

Figure 1a.

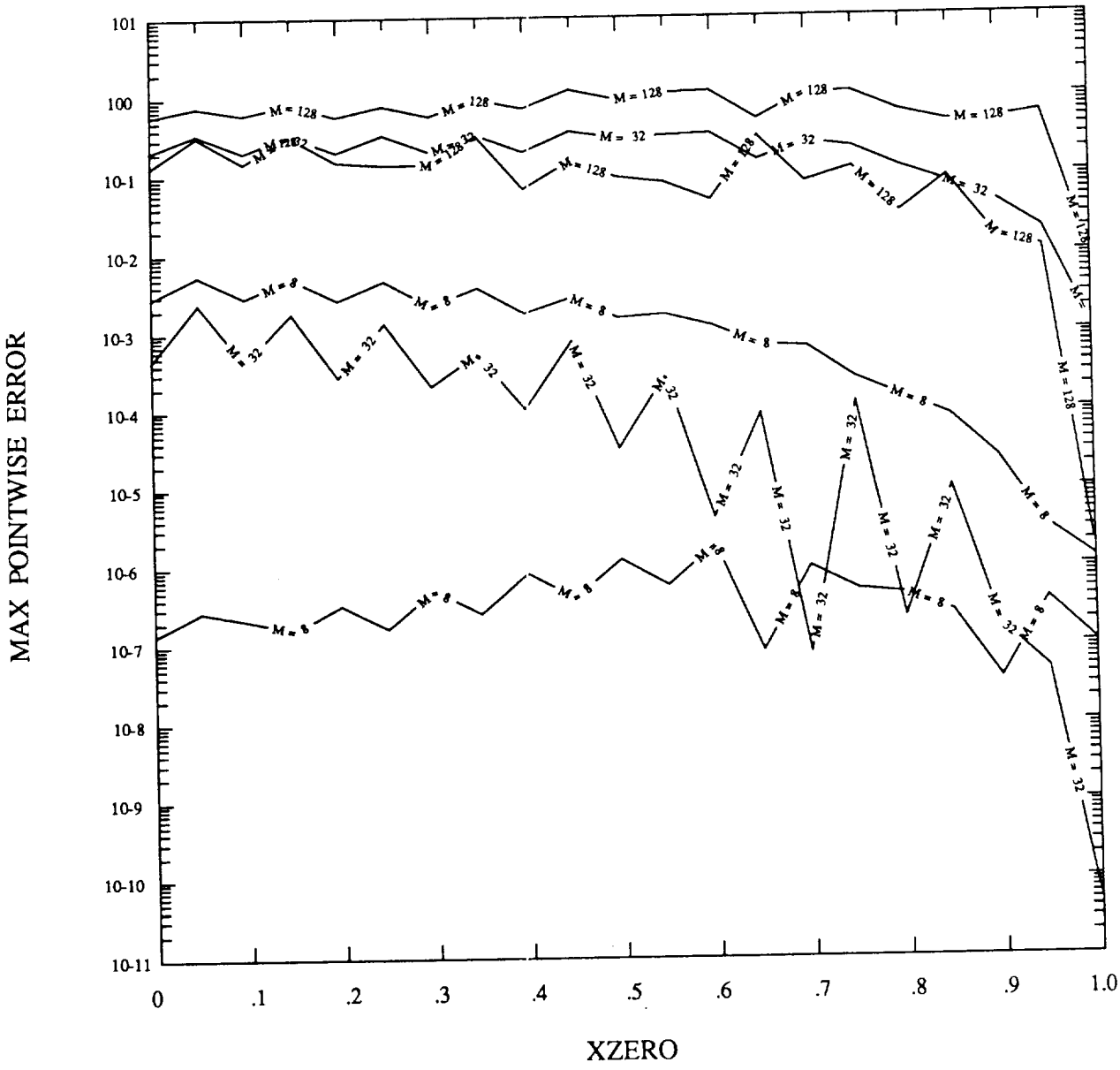
MAX POINTWISE ERROR
101
100
10-1
10-2
10-3
10-4
10-5
10-6
10-7
10-8
10-9
10-10
10-11
0
.1
.2
.3
.4
.5
.6
.7
.8
.9
1.0
XZERO
M = 128
M = 32
M = 8

Figure 1b.

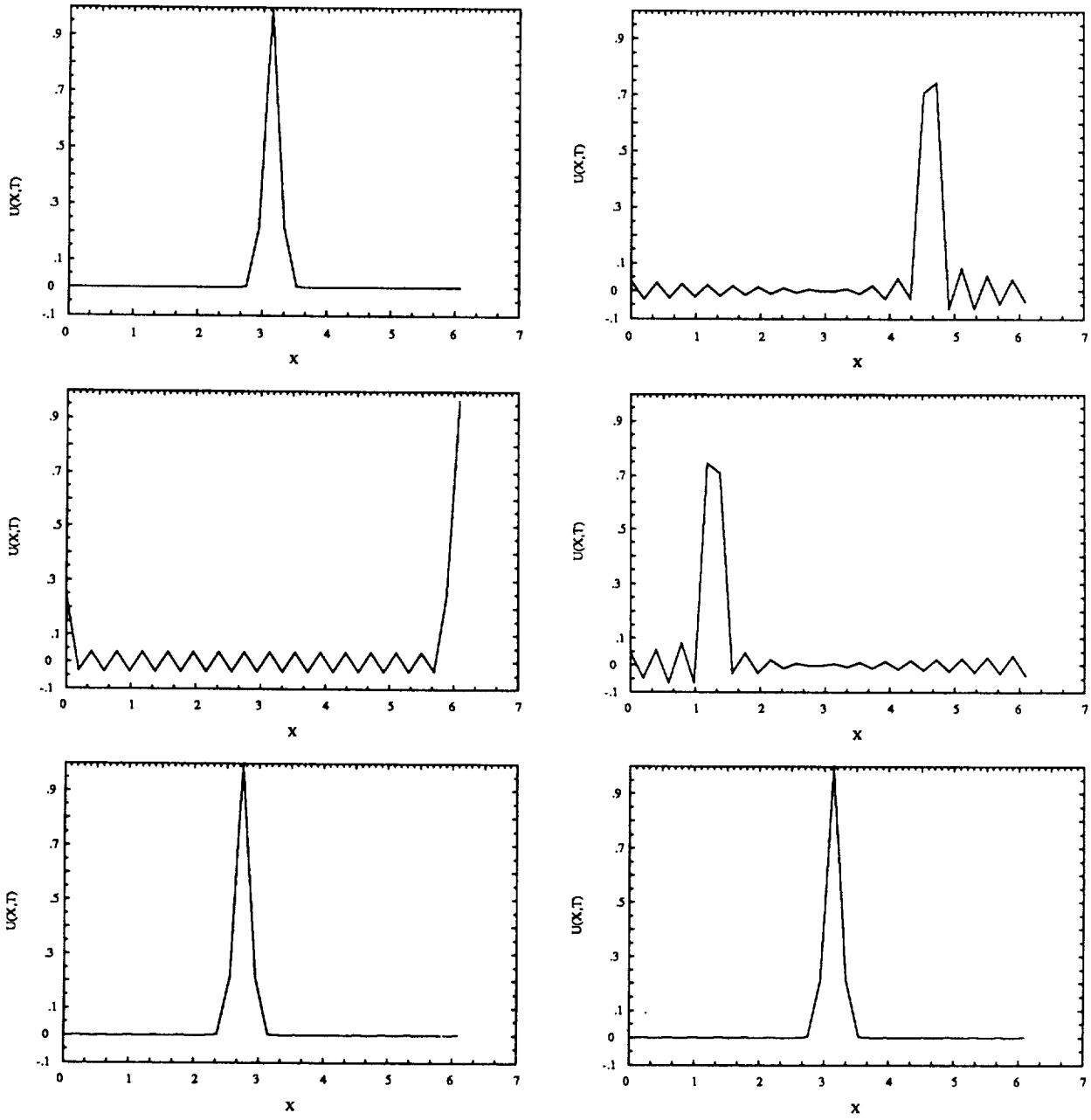

Figure 2a.

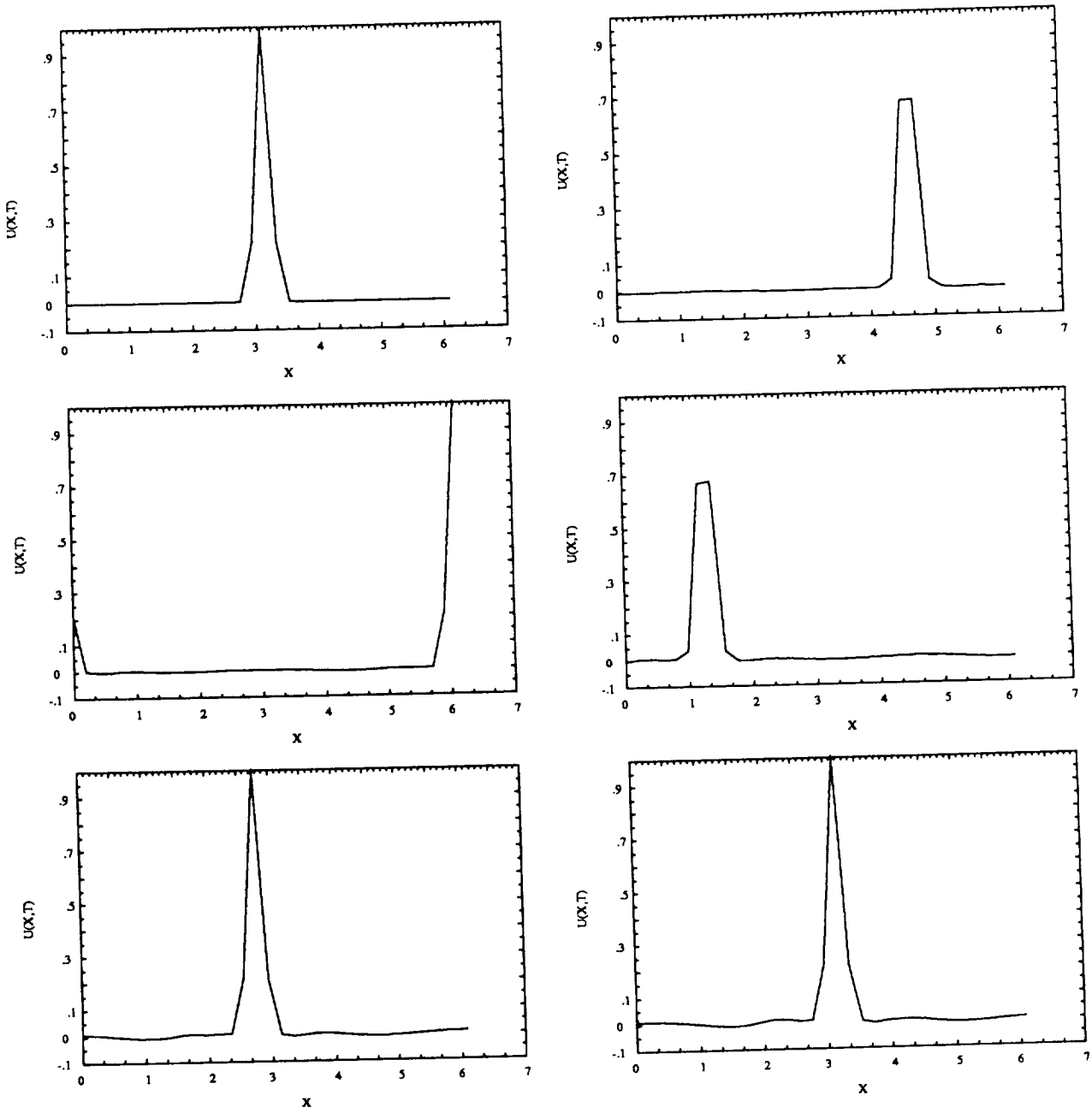

Figure 2b.

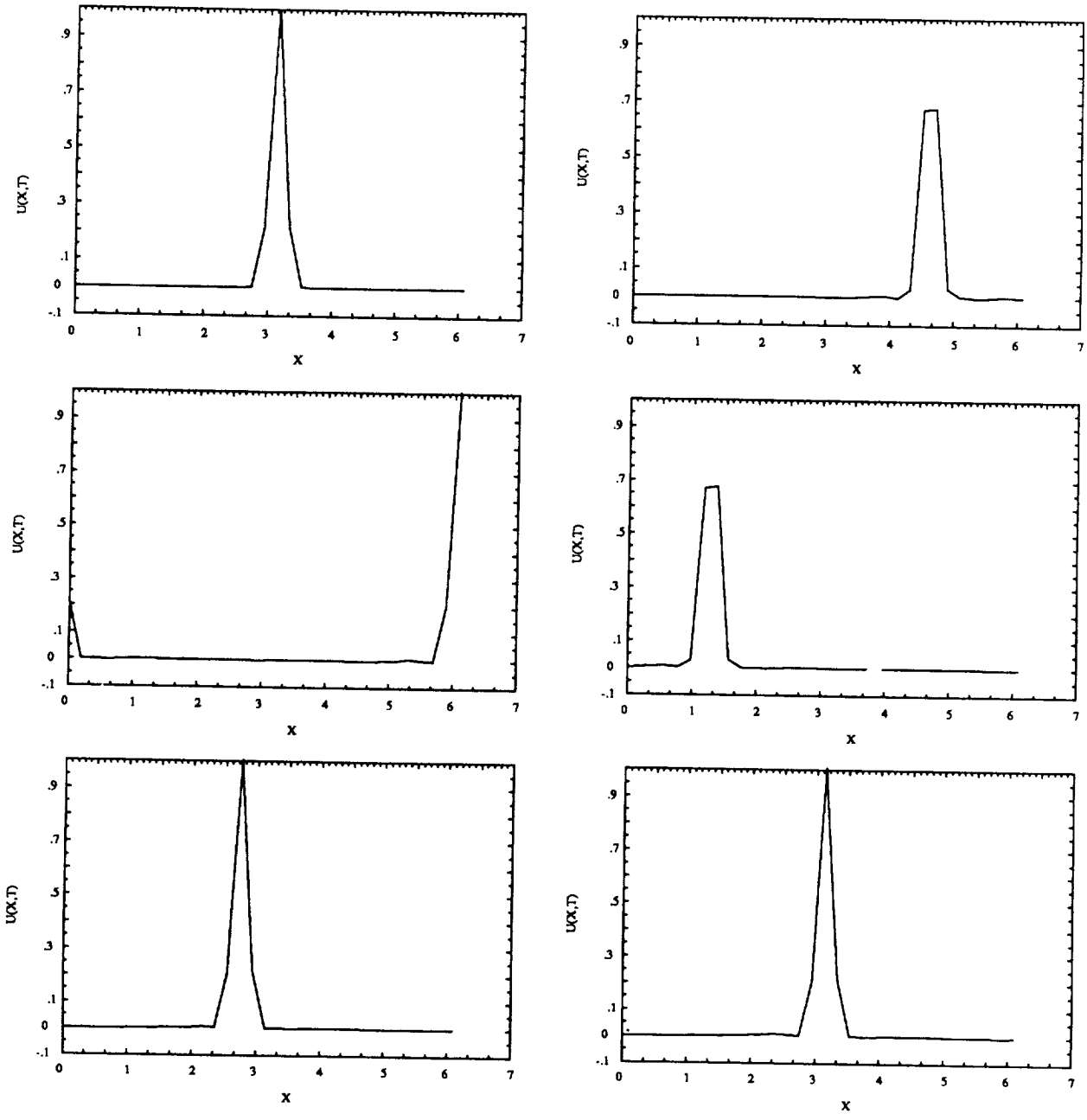

Figure 2c.

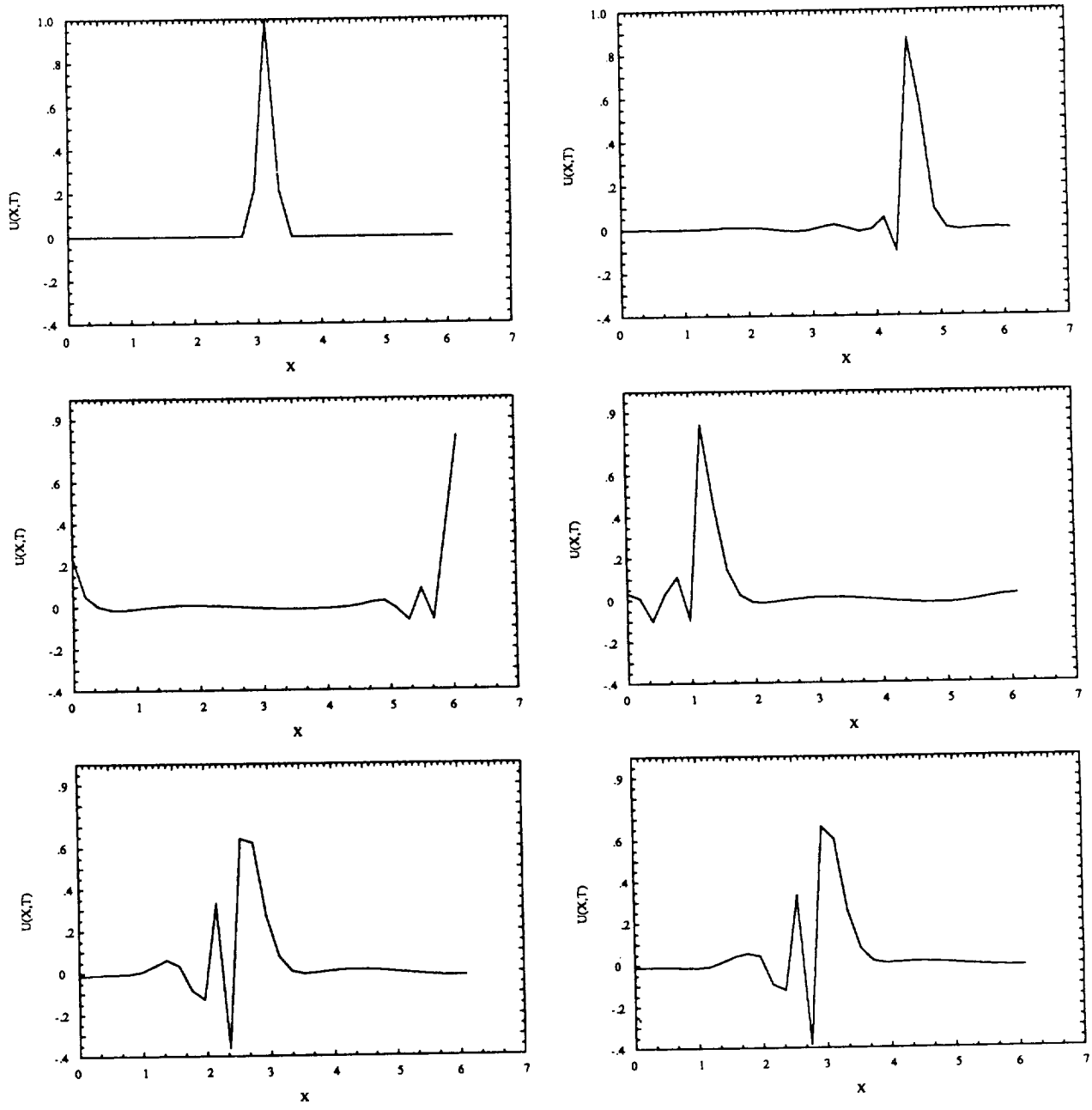

Figure 2d.

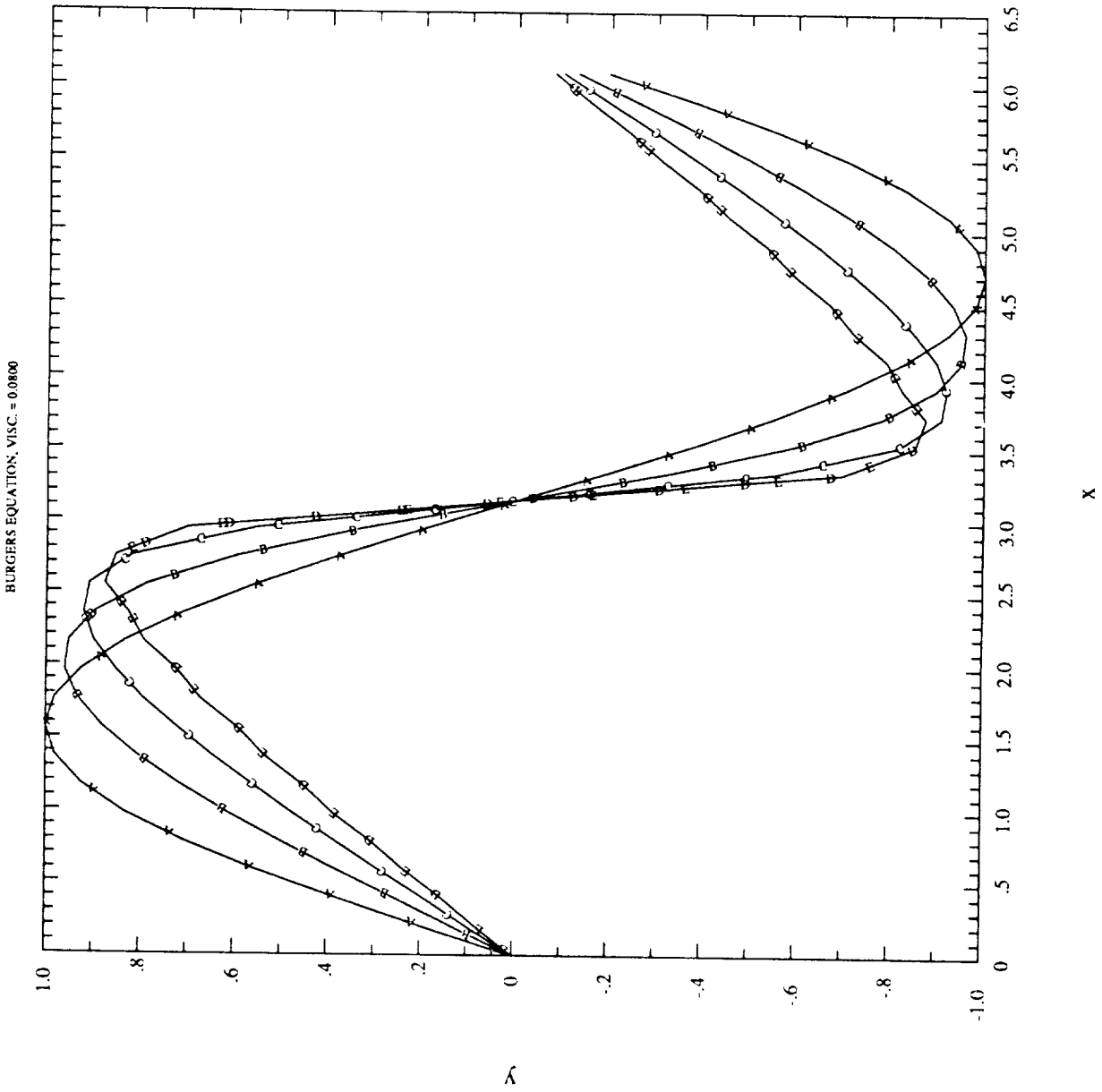
BURGERS EQUATION, VISC. = 0.0800
1.0
.8
.6
.4
.2
0
-.2
-.4
-.6
-.8
-1.0
y
0
.5
1.0
1.5
2.0
2.5
3.0
3.5
4.0
4.5
5.0
5.5
6.0
6.5
x

Figure 3a.

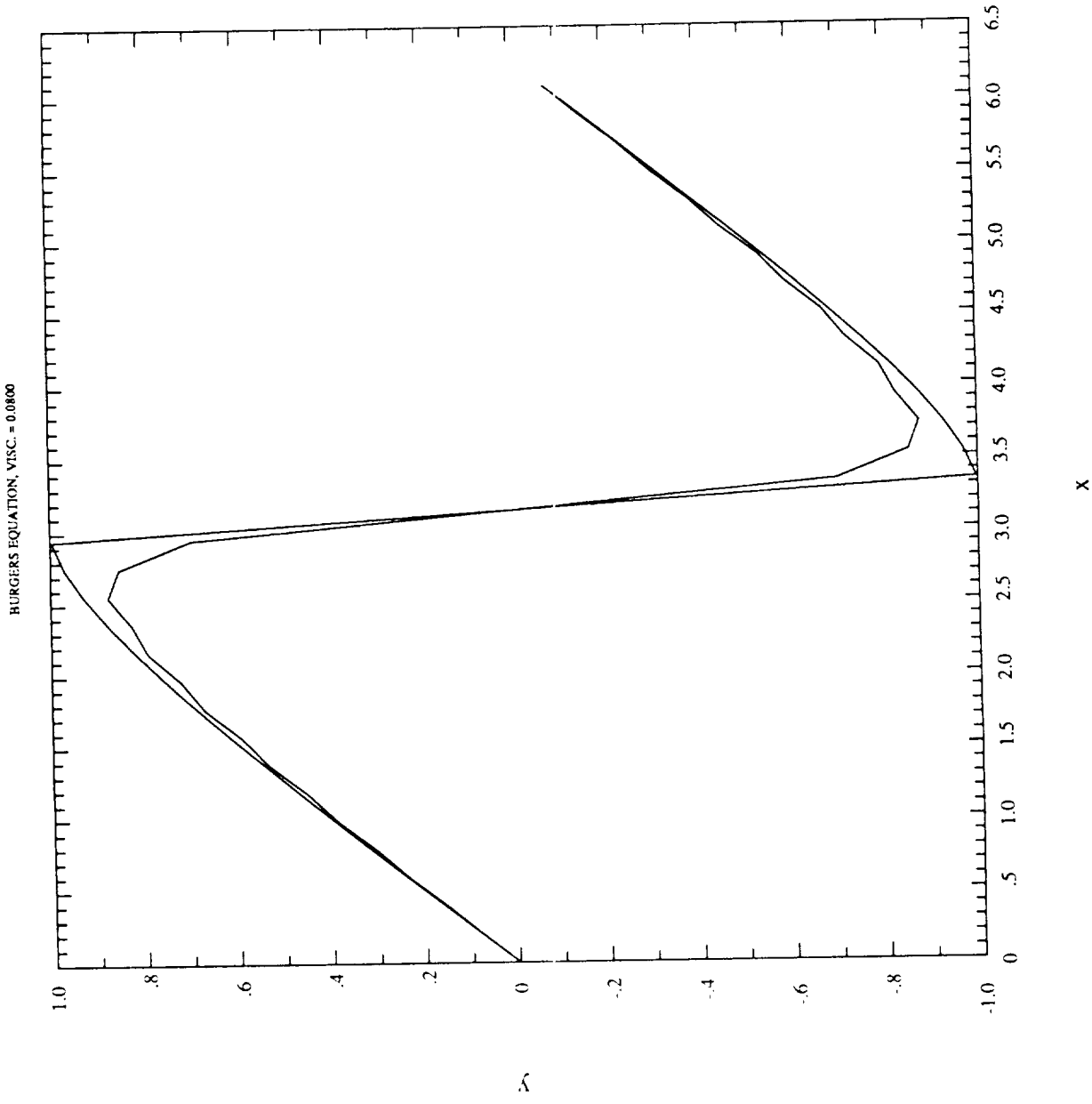
BURGERS EQUATION, VISC. = 0.0800
1.0
.8
.6
.4
.2
0
-.2
-.4
-.6
-.8
-1.0
0
.5
1.0
1.5
2.0
2.5
3.0
3.5
4.0
4.5
5.0
5.5
6.0
6.5
Y
X

Figure 3b.

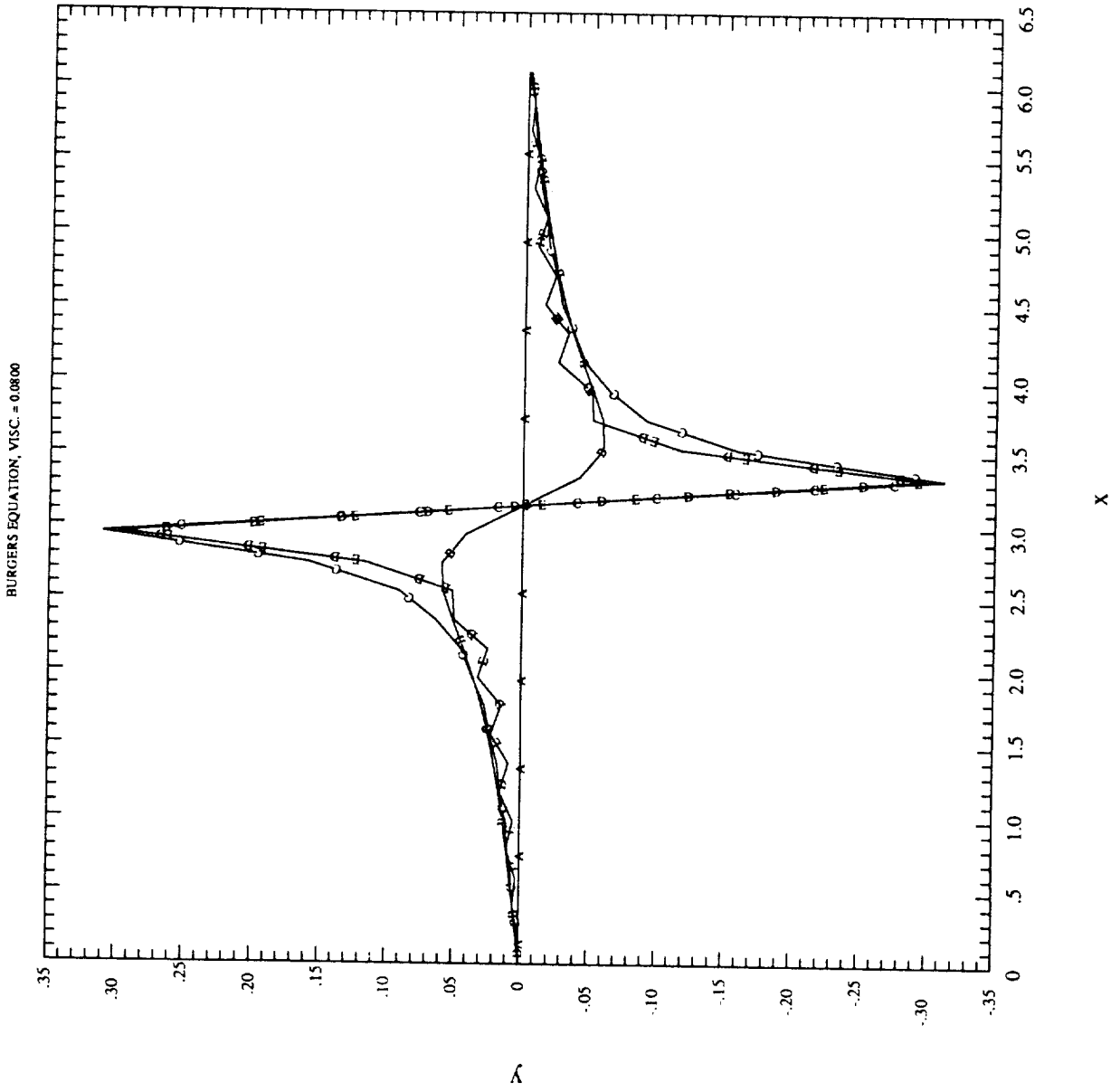
BURGERS EQUATION, VISC. = 0.0800
.35
.30
.25
.20
.15
.10
.05
0
-.05
-.10
-.15
-.20
-.25
-.30
-.35
0
.5
1.0
1.5
2.0
2.5
3.0
3.5
4.0
4.5
5.0
5.5
6.0
6.5
Y
X

Figure 3c.

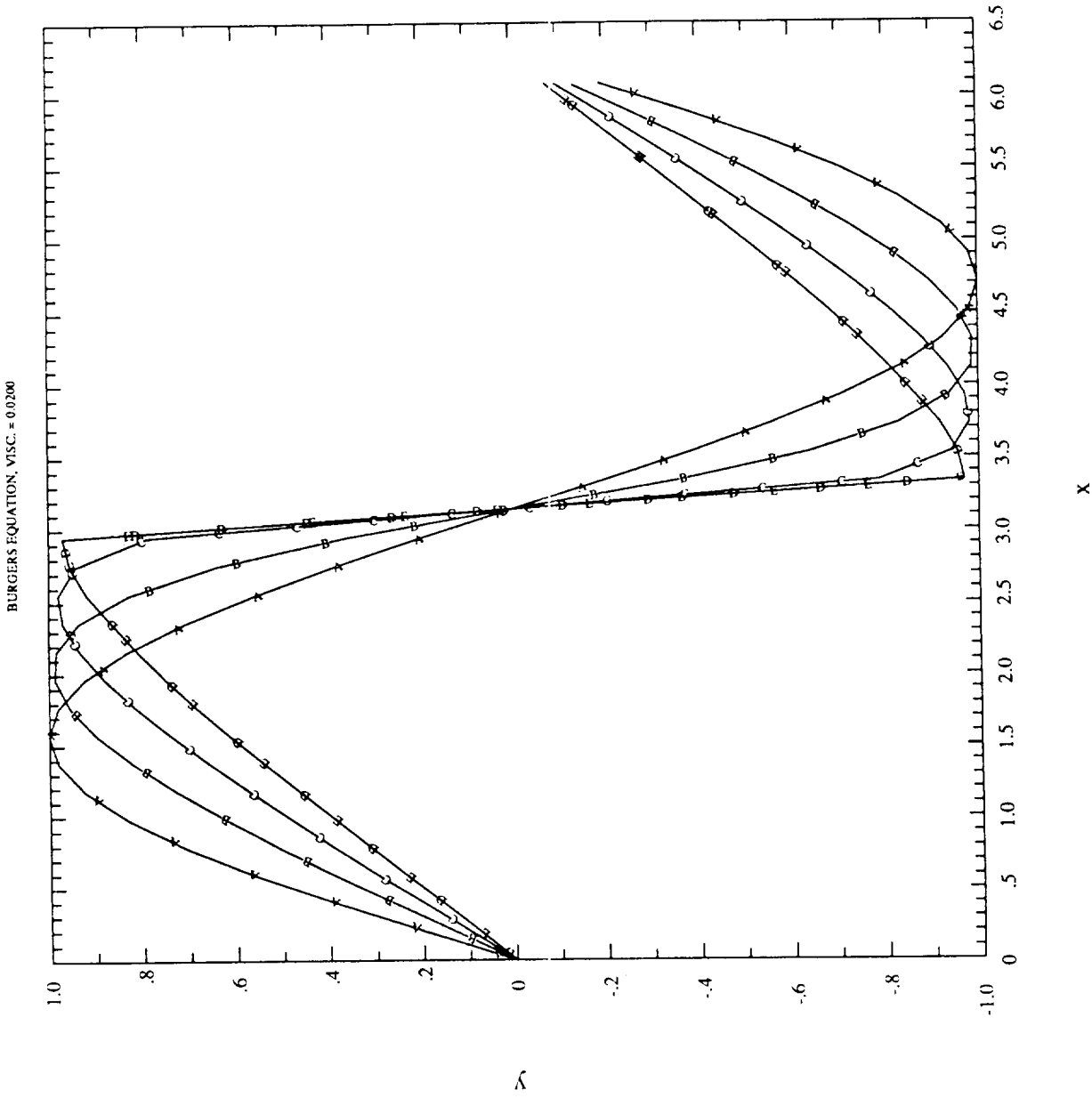
BURGERS EQUATION, VISC. = 0.0200
1.0
.8
.6
.4
.2
0
-.2
-.4
-.6
-.8
-1.0
0
.5
1.0
1.5
2.0
2.5
3.0
3.5
4.0
4.5
5.0
5.5
6.0
6.5
Y
X

Figure 4a.

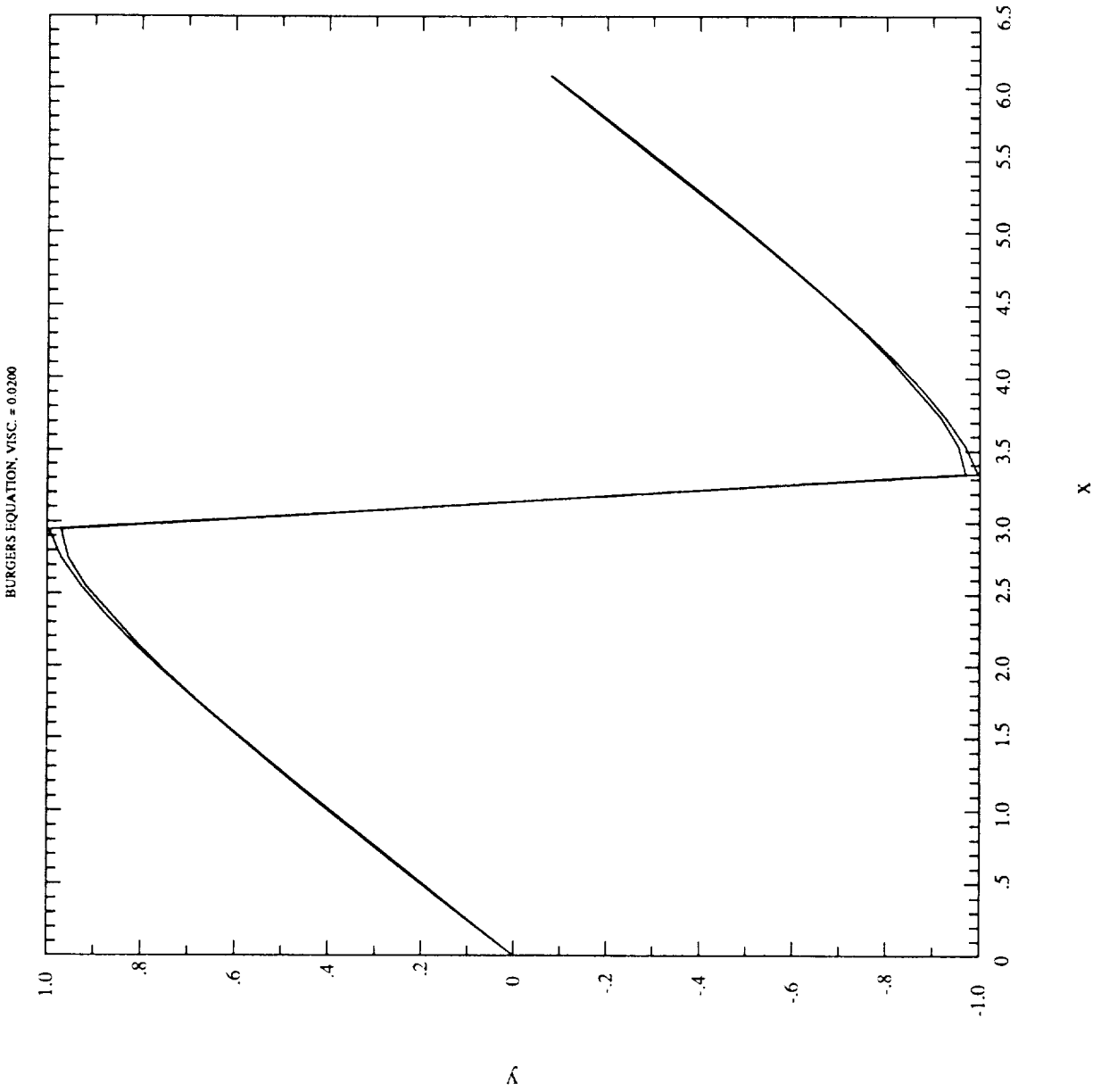
BURGERS EQUATION, VISC. = 0.0200
1.0
.8
.6
.4
.2
0
-.2
-.4
-.6
-.8
-1.0
Y
0
.5
1.0
1.5
2.0
2.5
3.0
3.5
4.0
4.5
5.0
5.5
6.0
6.5
X

Figure 4b.

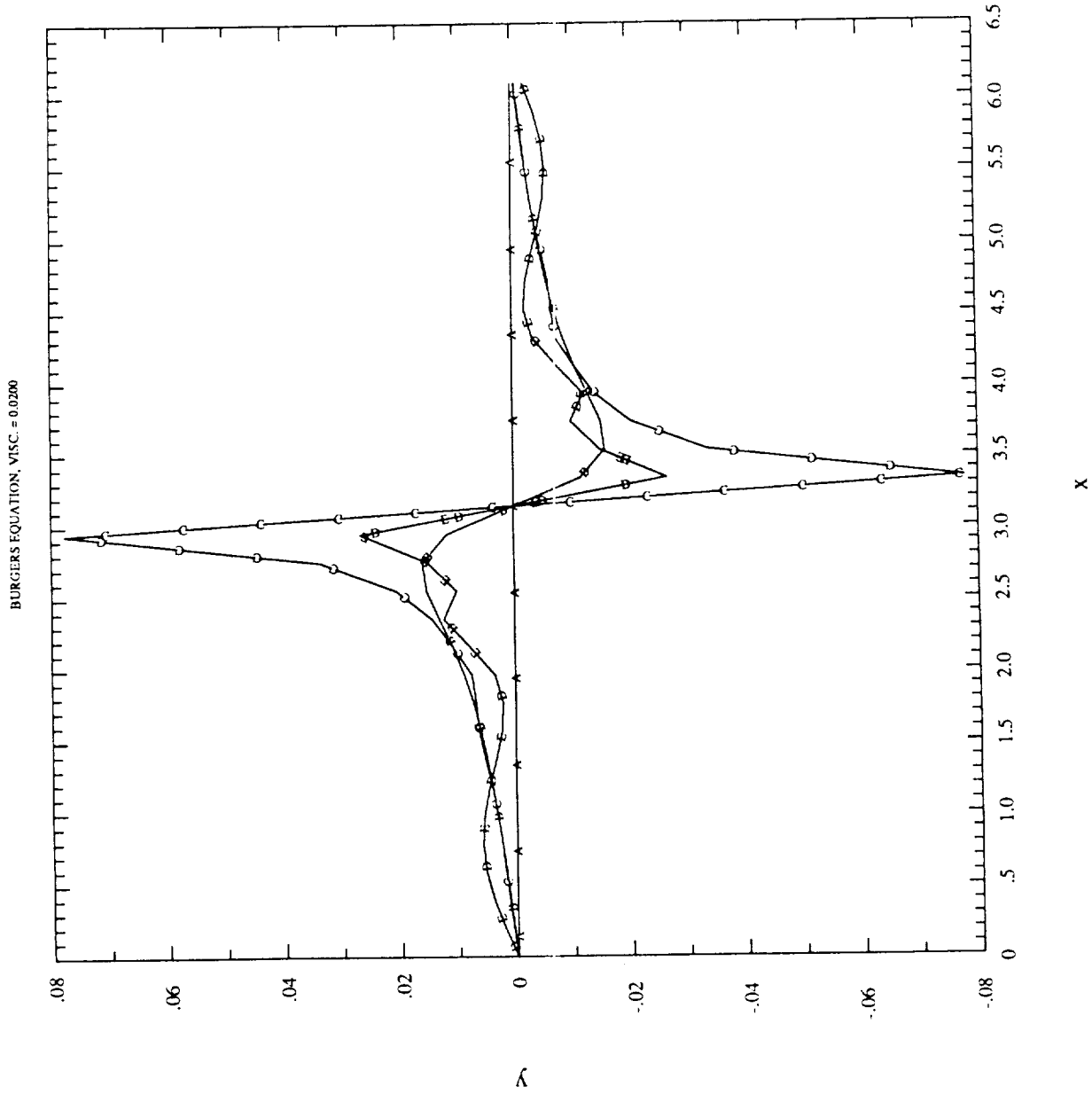
BURGERS EQUATION, VISC. = 0.0200
.08
.06
.04
.02
0
-.02
-.04
-.06
-.08
Y
0
.5
1.0
1.5
2.0
2.5
3.0
3.5
4.0
4.5
5.0
5.5
6.0
6.5
X

Figure 4c.

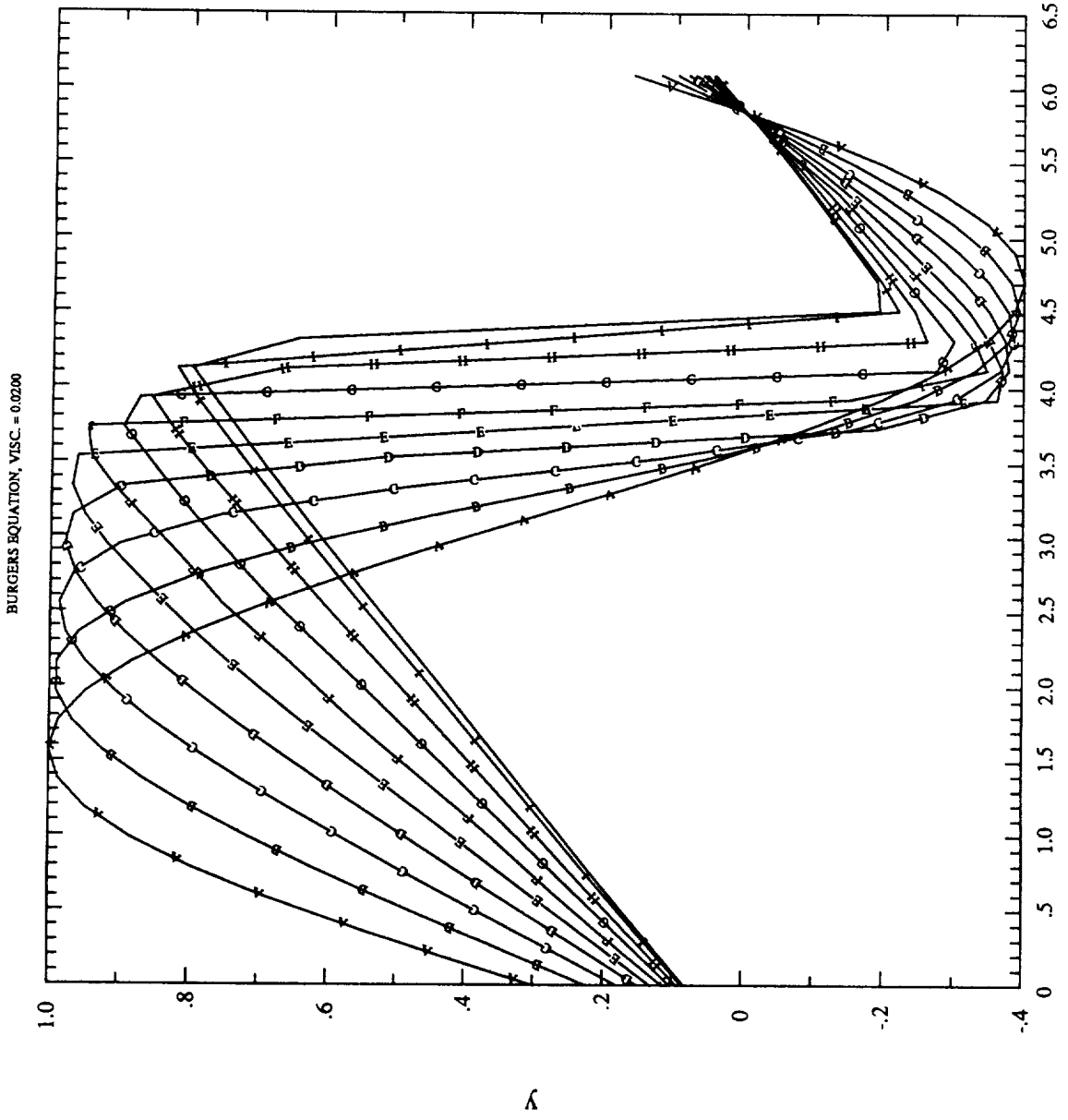
BURGERS EQUATION, VISC. = 0.0200
1.0
.8
.6
.4
.2
0
-.2
-.4
y
0
.5
1.0
1.5
2.0
2.5
3.0
3.5
4.0
4.5
5.0
5.5
6.0
6.5
x

Figure 5a.

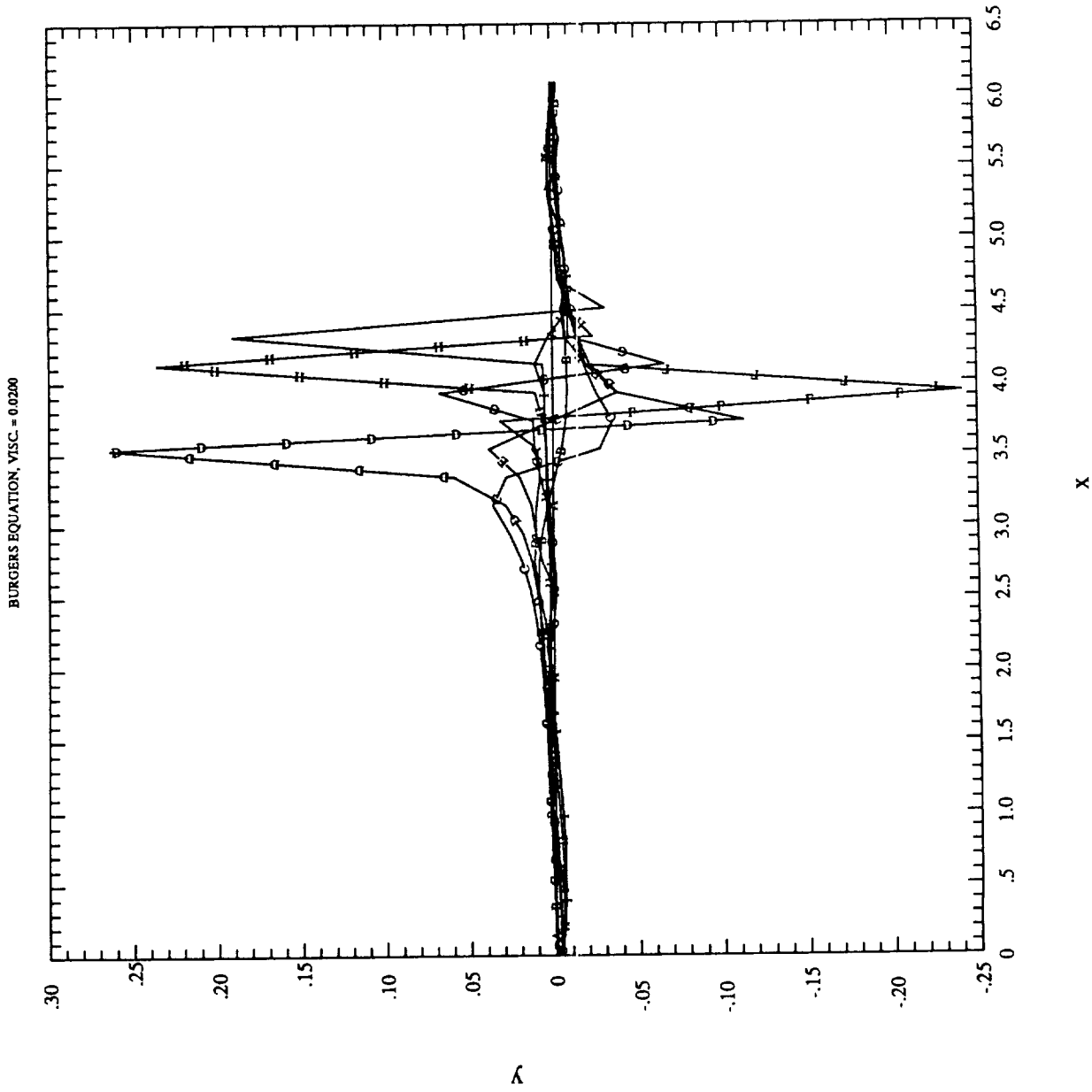
BURGERS EQUATION, VISC. = 0.0200
.30
.25
.20
.15
.10
.05
0
-.05
-.10
-.15
-.20
-.25
0
.5
1.0
1.5
2.0
2.5
3.0
3.5
4.0
4.5
5.0
5.5
6.0
6.5
X
Y

Figure 5b.

NASA
National Aeronautics and Space Administration

Report Documentation Page

1. Report No.	2. Government Accession No.	3. Recipient's Catalog No.
NASA CR-181717 ICASE Report No. 88-54		

4. Title and Subtitle	5. Report Date
AN ADAPTIVE PSEUDOSPECTRAL METHOD FOR DISCONTINUOUS PROBLEMS	September 1988
	6. Performing Organization Code

7. Author(s)	8. Performing Organization Report No.
Jeffrey M. Augenbaum	88-54
	10. Work Unit No.
	505-90-21-01

9. Performing Organization Name and Address	11. Contract or Grant No.
Institute for Computer Applications in Science and Engineering Mail Stop 132C, NASA Langley Research Center Hampton, VA 23665-5225	NAS1-18107
	13. Type of Report and Period Covered
12. Sponsoring Agency Name and Address	Contractor Report
National Aeronautics and Space Administration Langley Research Center Hampton, VA 23665-5225	14. Sponsoring Agency Code

15. Supplementary Notes

Langley Technical Monitor:
Richard W. Barnwell

To appear in Applied Numerical Mathematics

Final Report

16. Abstract

In this paper, we study the accuracy of adaptively chosen, mapped polynomial approximations for functions with steep gradients or discontinuities. We show that, for steep gradient functions, one can obtain spectral accuracy in the original coordinate system by using polynomial approximations in a transformed coordinate system with substantially fewer collocation points than are necessary using polynomial expansion directly in the original, physical, coordinate system. We also show that one can avoid the usual Gibbs oscillation, associated with steep gradient solutions of hyperbolic pde's, by approximation in suitably chosen coordinate systems. Continuous, high gradient, solutions are computed with spectral accuracy (as measured in the physical coordinate system). Discontinuous solutions associated with nonlinear hyperbolic equations can be accurately computed by using an artificial viscosity chosen to smooth out the solution in the mapped, computational, domain. Thus, we can effectively resolve shocks on a scale that is subgrid to the resolution available with collocation only in the physical domain. Examples with Fourier and Chebyshev collocation are given.

17. Key Words (Suggested by Author(s))	18. Distribution Statement
pseudospectral method, adaptive procedure	64 - Numerical Analysis Unclassified - unlimited

19. Security Classif. (of this report)	20. Security Classif. (of this page)	21. No. of pages	22. Price
Unclassified	Unclassified	33	A03